

Reexamining closed-form formulae for inclusive breakup: Application to deuteron and ${}^6\text{Li}$ induced reactions

Jin Lei^{1,*} and A. M. Moro^{1,†}

¹*Departamento de FAMN, Universidad de Sevilla, Apartado 1065, 41080 Sevilla, Spain.*

(Dated: April 3, 2018)

The problem of the calculation of inclusive breakup cross sections in nuclear reactions is reexamined. For that purpose, the post-form theory proposed by Ichimura, Austern and Vincent [Phys. Rev. C32, 431 (1985)] is revisited, and an alternative derivation of the non-elastic breakup part of the inclusive breakup is presented, making use of the coupled-channels optical theorem. Using the DWBA version of this model, several applications to deuteron and ${}^6\text{Li}$ reactions are presented and compared with available data. The validity of the zero-range approximation of the DWBA formula is also investigated by comparing zero-range with full finite-range calculations.

I. INTRODUCTION

The breakup of a nucleus into two or more fragments is an important mechanism occurring in nuclear collisions, particularly when one of the colliding nuclei is weakly bound. The analysis of this kind of processes has provided useful information on the structure of the broken nucleus, such as binding energies, spectroscopic factors and angular momentum (e.g. [1, 2]), and has contributed to the understanding of the dynamics of the reactions among composite systems.

In the simplest scenario, in which the projectile is broken up into two fragments, these processes can be schematically represented as $a + A \rightarrow b + x + A$, where $a = b + x$. From the theoretical point of view, this problem is difficult to treat because one has to deal with three-body final states. When the state of the three outgoing fragments (b , x and A) is fully determined, the reaction is said to be *exclusive*. If, in addition, the three particles are emitted in their ground state, the corresponding cross section is referred to as *elastic breakup* (EBU). In this case, the reaction can be treated as an effective three-body problem interacting via some effective two-body interactions. Although the rigorous formal solution of this problem is given by the Faddeev formalism [3, 4], the difficulty of solving these equations has led to the development of simpler approaches, such as the distorted-wave Born approximation (DWBA) [5], the continuum-discretized coupled-channels (CDCC) method [6] and a variety of semiclassical approaches [7–10].

A more complicated situation occurs when the final state of one or more fragments is not specified. In this case, the reaction is said to be *inclusive* with respect to this unobserved particle(s). This is the case of reactions of the form $a + A \rightarrow b + B^*$, where B^* is any possible configuration of the $x + A$ system. This includes the breakup processes in which x is elastically scattered by A , which corresponds to the EBU defined above, but also

breakup accompanied by target excitation, particle(s) exchange between x and A , x transfer to A , and the fusion of x by A , which are globally referred to as *non-elastic breakup* (NEB). The total inclusive breakup (TBU) will be therefore the sum of EBU and NEB components, i.e. $\text{TBU} = \text{EBU} + \text{NEB}$. Measured observables usually correspond to single or double differential cross sections with respect to the angle and/or energy of b and hence include both EBU and NEB contributions.

The evaluation of NEB cross sections are needed, for example, in the calculation of total fusion cross sections in reactions induced by weakly-bound projectiles (e.g. ${}^6\text{Li}$, ${}^7\text{Li}$, ${}^9\text{Be}$). A significant fraction of the total fusion cross section comes from incomplete fusion (ICF), in which only part of the projectile fuses with the target, the other fragment surviving after the collision [11]. Although many theoretical efforts have been made to develop suitable models to calculate ICF cross sections [12–14], the unambiguous calculation of CF and ICF within a fully quantum mechanical model remains a challenging problem [15, 16]. Because the ICF is part of the inclusive breakup, the study of inclusive breakup reactions may lead in turn to a better understanding of ICF.

A related problem is that of the indirect determination of neutron-induced cross sections on short-lived nuclei, from a surrogate reaction which gives rise to the same compound nucleus [17]. This is the case, for example, of the process $A(n, f)$ (where f is a fission fragment) for which the surrogate reaction $A(d, pf)$ may be used. To extract the cross section for the former, one needs to know the fraction of protons produced in the surrogate reaction which are accompanied by the formation of a $n + A$ compound nucleus. Therefore, the applicability of the method requires the separation of the EBU component (which does not lead to compound-nucleus formation) from the NEB (which contains the absorption cross section).

The calculation of inclusive breakup observables is more involved than that for the exclusive ones because they require the inclusion of all the possible processes through which the particle x can interact with the target A . Given the large number of accessible states, this

* jinlei@us.es

† moro@us.es

procedure is unpractical in most cases. As an alternative to this approach, one may try to replace the physical final states by a set of representative states (also named *doorway* states). These can be taken, for example, as the eigenstates of the $x + A$ Hamiltonian in a mean-field potential. As long as the basis used to describe these final states is complete, one may argue that the sum over these representative states should provide results close to those obtained if the sum were done over the true physical states. This procedure, referred to in some works as *transfer to the continuum* method, has been used recently with rather success to describe some inclusive breakup reactions of weakly-bound projectiles at Coulomb barrier energies, such as $^{208}\text{Pb}(^8\text{Li}, ^7\text{Li})$ [18], $^{208}\text{Pb}(^6\text{He}, \alpha)$ [19], and $^{120}\text{Sn}(^6\text{He}, \alpha)$ [20]. However, despite this relative success, this method is based on a heuristic approach rather than on a rigorous formal theory. Lacking this formal justification, it is not clear how these *doorway* states should be chosen and how the final calculated cross sections depend on this choice. Another drawback of this approach is that it does not allow to separate the contributions coming from EBU and NEB.

At intermediate energies (above ~ 100 MeV/u), the problem can be greatly simplified using the *adiabatic* (fast collision) and *eikonal* (forward scattering) approximations, which allows to obtain closed formulas of the inclusive process in terms of the absorption and survival probabilities of the unobserved particle as a function of the impact parameter. This approach has been used extensively in the analysis of nucleon removal (knockout) experiments at intermediate energies, in which typically the removed particle is not observed and only the momentum distributions of the residual core is measured (see, e.g. Refs. [21, 22] and references therein). These models, however, cannot be applied to low incident energies (a few MeV/u) and when the energy/momentum transfer is large.

The problem of the calculation of inclusive breakup cross sections is nevertheless not new. This problem was studied in detail by some groups since the late seventies, and several theories were proposed and applied. The aim of these theories was to derive closed-form formulas, in which the sum over final states of the $x + A$ system is formally reduced to some expectation value of the imaginary part of the $x + A$ optical potential. In the pioneering works by Baur and co-workers [23–25], the sum is done making use of unitarity and a surface approximation of the form factors of excited states of the residual nucleus. These two approximations were avoided in later works by Udagawa and Tamura [26, 27], who used a prior-form DWBA formalism, and by Austern and Vincent [28], who used the post-form DWBA. The latter was refined by Kasano and Ichimura [29], who found a formal separation between the EBU and NEB contributions. These results were carefully reviewed by Ichimura, Austern and Vincent [30] and the model was subsequently referred to as the IAV formalism. Later on, Austern *et al.* reformulated this theory within a more complete three-body

model [6].

It is worth noting that the prior-form model of Udagawa and Tamura (UT), on one side, and the post-form DWBA model of Austern and Vincent (AV), on the other side, although formally similar, give different predictions for the NEB part. This led to a long-standing dispute between these two groups, which was finally settled in the referred IAV work [30], where it was demonstrated that a proper derivation of the prior-form formula gives rises to additional terms not considered by UT.

Although the comparison of these theories with experimental data showed very encouraging results, they have apparently fallen into disuse. Moreover, some of these theories, such as the three-body model of Austern, has never been tested to our knowledge, probably due to the computational limitations at that time. This is in contrast to the experimental situation, in which inclusive breakup measurements are used for many applications, with both stable and unstable beams. Therefore, it seems timely to reexamine these theories and study their applicability to problems of current interest.

The revival and increasing interest on this problem is evidenced by two recent theoretical works on this subject [31, 32]. Both of them use the IAV model, in DWBA. In Ref. [31], the authors use the zero-range post-form of this model, whereas in Ref. [32] the finite-range prior-form version of the model is used instead. Both of them apply the method to deuteron induced reactions, with encouraging results.

In this paper, we revisit also the IAV model, with special emphasis on the calculation of the NEB part, for which we provide a new derivation. We have implemented the DWBA version of this model both in zero-range and in exact finite-range. To assess the validity of this theory, we have performed calculations for several reactions induced by deuterons and, for the first time, the method is applied to ^6Li scattering. In both cases, we compare with available data.

The paper is organized as follows. In Sec. II we give a short overview of the theory, including a new derivation of the NEB formula within the IAV model. In Sec. III, the formalism is applied to several inclusive reactions induced by deuterons and ^6Li . Finally, in Sec. IV we summarize the main results of this work and outline some future developments.

II. THE ICHIMURA, AUSTERN, VINCENT (IAV) MODEL

In this section we briefly review the model of Ichimura, Austern and Vincent [6, 30]. The final formula obtained in this model has been derived in different ways. Here, we closely follow the early derivation done by Austern and Vincent [28] because it provides an interesting physical insight.

We write the process under study as

$$a(= b + x) + A \rightarrow b + B^*. \quad (1)$$

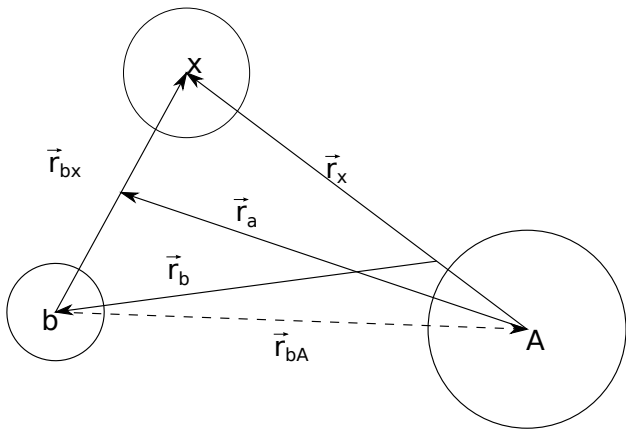


FIG. 1. Coordinates used in the breakup reaction.

This process will be described with the Hamiltonian

$$H = K + V_{bx} + U_{bA}(\vec{r}_{bA}) + H_A(\xi) + V_{xA}(\xi, \vec{r}_x), \quad (2)$$

where K is the total kinetic energy operator, V_{bx} is the interaction binding the two clusters b and x in the projectile a , $H_A(\xi)$ is the Hamiltonian of the target nucleus (with ξ denoting its internal coordinates) and V_{xA} and U_{bA} are the fragment–target interactions. The relevant coordinates are depicted in Fig. 1. Note that the coordinate \vec{r}_b connects the particle b with the center of mass (c.m.) of the $x + A$ system.

In writing the Hamiltonian of the system in the form (2) we make a clear distinction between the two cluster constituents; the interaction of the fragment b , the one that is assumed to be detected in the experiment, is described with an optical potential. Non-elastic processes arising from this interaction (e.g. target excitation), are included only effectively through U_{bA} . The particle b is said to act as *spectator*. On the other hand, the interaction of the particle x with the target retains the dependence of the target degrees of freedom (ξ).

Within the assumed three-body model, and using the post-form representation, the total wave function of the system can be written in integral form as

$$\Psi(\xi, \vec{r}_x, \vec{r}_b) = [E^+ - K_b - U_{bB} - H_B]^{-1} \times V_{\text{post}} \Psi(\xi, \vec{r}_x, \vec{r}_b), \quad (3)$$

where $E^+ = E + i\epsilon$, $\epsilon \rightarrow 0$, U_{bB} is an auxiliary (and, in principle, arbitrary) potential between b and the composite B , $V_{\text{post}} \equiv V_{bx} + U_{bA} - U_{bB}$ and H_B is the Hamiltonian of the $x+A$ pair, given by

$$H_B(\xi, \vec{r}_x) = H_A(\xi) + K_x + V_{xA}(\xi, \vec{r}_x). \quad (4)$$

The eigenstates of the target Hamiltonian will be denoted as $\phi_A^c(\xi)$, i.e., $[H_A(\xi_A) - E_A^c] \phi_A^c(\xi) = 0$, with $c = 0$ corresponding to the target ground state, for which we assume $E_A^0 = 0$.

We consider now a specific final state of the detected particle b , characterized by a given final momentum of this fragment (\vec{k}_b). The motion of b will be described by a distorted wave with momentum \vec{k}_b , obtained as a solution of the single-channel equation

$$[K_b + U_{bB}^\dagger - E_b] \chi_b^{(-)}(\vec{k}_b, \vec{r}_b) = 0. \quad (5)$$

The wave function describing the motion of x after the breakup, that will be denoted as $Z_x(\xi, \vec{r}_x)$, can be obtained projecting the total wave function [Eq. (3)] onto this particular state of the b particle, i.e.,¹

$$Z_x(\vec{k}_b, \xi, \vec{r}_x) \equiv (\chi_b^{(-)}) |\Psi\rangle = [E^+ - E_b - H_B]^{-1} (\chi_b^{(-)} |V_{\text{post}} |\Psi\rangle), \quad (6)$$

where the round bracket denotes integration over \vec{r}_b only. The last equation can be also written in differential form as

$$[E^+ - E_b - H_B] Z_x(\vec{k}_b, \xi, \vec{r}_x) = (\chi_b^{(-)} |V_{\text{post}} |\Psi\rangle). \quad (7)$$

The source term of this equation involves the exact and hence unknown wave function Ψ which, in actual calculations, must be approximated by some calculable form. For example, in DWBA, one assumes the factorized form

$$\Psi(\xi, \vec{r}_x, \vec{r}_b) \approx \phi_A^0(\xi) \phi_a(\vec{r}_{bx}) \chi_a^{(+)}(\vec{k}_a, \vec{r}_a), \quad (8)$$

where $\phi_a(\vec{r}_{bx})$ is the projectile ground-state wave function and $\chi_a^{(+)}(\vec{k}_a, \vec{r}_a)$ is a distorted wave describing the $a + A$ motion in the incident channel. In practice, the latter is commonly replaced by the solution of some optical potential describing $a + A$ elastic scattering. Austern *et al.* [6] proposed also the three-body approximation

$$\Psi(\xi, \vec{r}_x, \vec{r}_b) \approx \phi_A^0(\xi) \Psi^{3b}(\vec{r}_x, \vec{r}_b), \quad (9)$$

where Ψ^{3b} is a three-body wave function for the three fragments ($x+b+A$) and contains, in addition to the $b+x$ ground state, contributions from $b+x$ inelastic scattering and breakup.

It is worth noting that, either in the approximation (8) or in (9), the three-body wave function does not contain explicitly excited states of A . Thus, in the IAV model, the NEB can be viewed as a two-step process in which the first step is the dissociation of the projectile, leaving the target in the ground state, while the second step is the absorption of x or the excitation of A .

A possible procedure to solve Eq. (7) is to expand the function Z_x in a complete set of $x + A$ states, i.e.,

$$Z_x(\vec{k}_b, \xi, \vec{r}_x) = \sum_c \psi_x^c(\vec{k}_b, \vec{r}_x) \phi_A^c(\xi), \quad (10)$$

¹ Note that this function will also depend on \vec{k}_a , which indicates the direction of the incident beam. Because this direction is fixed, this dependence will be omitted for simplicity of the notation.

where $\psi_x^c(\vec{k}_b, \vec{r}_x)$ describes the $x-A$ relative motion when the target is in the state c . The expansion (10) can be inserted into Eq. (7), giving rise to a set of coupled equations for the unknown functions $\psi_x^c(\vec{k}_b, \vec{r}_x)$.

This approach will be in general unpractical because the expansion (10) involves a very large number of final states. If one is not interested in the description of the transition to specific $x+A$ states, but rather in their summed contribution, one can proceed as follows. Following Feshbach, the $Z_x(\vec{k}_b, \xi, \vec{r}_x)$ function is decomposed as

$$Z_x(\vec{k}_b, \xi, \vec{r}_x) = \mathcal{P}Z_x + \mathcal{Q}Z_x, \quad (11)$$

where \mathcal{P} is the projector operator onto the target ground state and $\mathcal{Q} = 1 - \mathcal{P}$. From Eq. (10) we see that $\mathcal{P}Z_x = \psi_x^0(\vec{k}_b, \vec{r}_x)\phi_A^0(\xi)$. The function $\psi_x^0(\vec{k}_b, \vec{r}_x)$, which describes the $x+A$ relative motion when the target is in the ground state, verifies the equation

$$(E_x^+ - K_x - \mathcal{U}_x)\psi_x^0(\vec{k}_b, \vec{r}_x) = \rho(\vec{k}_b, \vec{r}_x) \quad (12)$$

with $E_x = E - E_b$, $\rho(\vec{k}_b, \vec{r}_x) \equiv (\chi_b^{(-)}|V_{bx}|\Psi)$ is the so-called source term, and \mathcal{U}_x the formal optical model potential describing $x+A$ elastic scattering. Explicitly,

$$\mathcal{U}_x = \langle \phi_A^0 | V_{xA} + V_{xA}\mathcal{Q}[E^+ - E_b - H_{QQ}]^{-1}V_{xA} | \phi_A^0 \rangle, \quad (13)$$

where $H_{QQ} \equiv \mathcal{Q}H_B\mathcal{Q}$. The formal potential \mathcal{U}_x is a complicated non-local, angular- and energy-dependent object. However, as done in two-body scattering problems, it can be approximated by some energy-averaged (possibly local) potential or by some phenomenological representation (denoted U_x hereafter) with parameters adjusted to describe $x+A$ elastic scattering.

Note that Eq. (12) is formally analogous to the inhomogeneous equation appearing in DWBA and CCBA calculations between bound states, as formulated in the *source term method* of Ascutto and Glendenning [33], and used by several coupled-channels codes [34].

A. Separation of elastic and nonelastic breakup

In their original paper, Austern and Vincent provide only the total inclusive cross section. Later on, Kasano and Ichimura [29] showed that this expression can be formally decomposed into two pieces, corresponding to the elastic breakup (EBU) and non-elastic breakup (NEB) contributions.

Here, we present an alternative derivation of these formulas, which exploits the aforementioned analogy of Eq. (12) with that found in the DWBA and CCBA formalisms. This equation is to be solved with purely outgoing boundary conditions (since there are no incoming waves in the $x-A$ channel), that is,

$$\psi_x^0(\vec{k}_b, \vec{r}_x) \rightarrow f(\vec{k}_b, \hat{r}_x) \frac{e^{ik_x r_x}}{r_x}. \quad (14)$$

The function $f(\vec{k}_b, \hat{r}_x)$ depends, in addition to the direction of \vec{k}_b , on the angular part of \vec{r}_x . Asymptotically, when r_x is large, the position vector \vec{r}_x becomes parallel to the momentum \vec{k}_x and we may write $f(\vec{k}_b, \hat{r}_x) \rightarrow f(\vec{k}_b, \vec{k}_x)$. We therefore recognize $f(\vec{k}_b, \vec{k}_x)$ as the scattering amplitude for the elastic breakup process, and its square is proportional to the differential cross section for the detection of the x particle in the direction of \vec{k}_x , and the b particle in the direction \vec{k}_b . To obtain this amplitude, one can proceed in two different ways. One possibility is to integrate the differential equation (12) and, at a sufficiently large distance (beyond the range of the short-ranged potentials), equate the solution to the asymptotic form (14), from which the scattering amplitude can be obtained. A second approach to solve Eq. (12) is to use integral methods (Green function) techniques. This gives a closed-form expression for the scattering amplitude,

$$f(\vec{k}_b, \vec{k}_x) = -\frac{\mu_x}{2\pi\hbar^2} \langle \chi_x^{(-)} \chi_b^{(-)} | V_{bx} | \Psi^{3b} \rangle, \quad (15)$$

where μ_x is the reduced mass of the $x+A$ system and the distorted wave $\chi_x^{(-)}(\vec{k}_x, \vec{r}_x)$ is a solution of the homogeneous part of equation Eq. (12), i.e.,

$$[K_x + U_x^\dagger - E_x] \chi_x^{(-)}(\vec{k}_x, \vec{r}_x) = 0, \quad (16)$$

whose solution consists of a plane wave of momentum \vec{k}_x plus an ingoing spherical wave.

The corresponding differential cross section, for a final differential volume in momentum space, is given by² (c.f., for instance, Eq. (5.36) of Ref. [35])

$$d\sigma = \frac{(2\pi)^{-5}}{\hbar v_i} \int d\vec{k}_x d\vec{k}_b d\vec{k}_A \delta(E_f - E_i) \delta(\vec{P}_f - \vec{P}_i) |T_{fi}|^2, \quad (17)$$

where T_{fi} is the usual transition amplitude (or T-matrix), which is related to the scattering amplitude by $f = -(\mu_x/2\pi\hbar^2)T_{fi}$. In the c.m. frame, $\vec{P}_i = 0$. Also, the target momentum (\vec{k}_A) is not measured, so we can integrate over it, making use of the momentum-conserving delta function,

$$d\sigma = \frac{(2\pi)^{-5}}{\hbar v_i} \int d\vec{k}_x d\vec{k}_b \delta(E_f - E_i) |T_{fi}|^2. \quad (18)$$

The element $d\vec{k}_b$ is conveniently expressed in terms of energy and solid angle elements using $d\vec{k}_b = (2\pi)^3 \rho_b(E_b) d\Omega_b dE_b$, where $\rho_b(E_b) = k_b \mu_b / ((2\pi)^3 \hbar^2)$ is

² Note that the factor $(2\pi)^4$ of Ref. [35] is replaced here by a $(2\pi)^{-5}$ factor, consistent with our definition of the amplitude for the plane waves as $e^{i\vec{k}\vec{r}}$.

the density of states.³ Using this in Eq. (18),

$$d\sigma = \frac{(2\pi)^{-2}}{\hbar v_i} \int \delta(E_f - E_i) |T_{fi}|^2 \rho_b(E_b) d\Omega_b dE_b d\vec{k}_x. \quad (19)$$

The double differential cross section with respect to the energy and the scattering angle of b is therefore given by

$$\left. \frac{d^2\sigma}{d\Omega_b dE_b} \right|_{\text{EBU}} = \frac{(2\pi)^{-2}}{\hbar v_i} \rho_b(E_b) \int \delta(E_f - E_i) |T_{fi}|^2 d\vec{k}_x, \quad (20)$$

which coincides with the result of Austern *et al.* (Eq. (8.15) of Ref. [6]) noting that $\int d\vec{k}_x \rightarrow (2\pi)^3 \sum_{\vec{k}_x}$.

Although it is not the purpose of the present work, we note also that the previous expression can be used to compute the fully exclusive cross section, with respect to the angles and energies of b and x . For that, we use again $d\vec{k}_x = (2\pi)^3 \rho_x(E_x) d\Omega_x dE_x$ and use the energy-conserving delta function, resulting

$$\left. \frac{d^2\sigma}{d\Omega_b dE_b d\Omega_x} \right|_{\text{EBU}} = \frac{2\pi}{\hbar v_i} \rho_b(E_b) \rho_x(E_x) |T_{fi}|^2. \quad (21)$$

To obtain the expression for the NEB component we make use of the *coupled-channels optical theorem* recently formulated by Cotanch [36]. This work generalizes the well-known optical theorem to the multichannel case. If χ_i is the channel wave function and W_i the diagonal imaginary part for this channel, the contribution to the absorption in this particular channel is given by [36]

$$\sigma_{\text{abs}}^i = -\frac{2}{\hbar v_{el}} \langle \chi_i | W_i | \chi_i \rangle, \quad (22)$$

where v_{el} is the projectile–target relative velocity in the incident (elastic) channel.

We may use this result to calculate the NEB contribution by noting that the latter is nothing but the absorption occurring in the $x + A$ channel. The channel wave function is given by $\psi_x^0(\vec{k}_b, \vec{r}_x)$, which is a solution of Eq. (12). Since Eq. (12) corresponds to a definite energy and direction of the b particle, we consider the differential cross section corresponding to a range of the outgoing momenta of b ,

$$d^2\sigma = -\frac{2}{\hbar v_i} \langle \psi_x^0 | W_x | \psi_x^0 \rangle N(k_b) d\vec{k}_b, \quad (23)$$

with $W_x \equiv \text{Im}[U_x]$. Transforming the element of momentum into energy and solid angle elements, we get the double differential cross section

$$\left. \frac{d^2\sigma}{dE_b d\Omega_b} \right|_{\text{NEB}} = -\frac{2}{\hbar v_i} \rho_b(E_b) \langle \psi_x^0 | W_x | \psi_x^0 \rangle. \quad (24)$$

³ These expressions result from $N(k)d\vec{k}_b = \rho_b(E_b)d\Omega_b dE_b$, where $N(k)$ is the number of states in the differential volume $d\vec{k}_b$, which is determined from $\langle \vec{k} | \vec{k}' \rangle = \delta(\vec{k} - \vec{k}') / N(k)$. In our case, $\langle \vec{k} | \vec{k}' \rangle = (2\pi)^3 \delta(\vec{k} - \vec{k}')$, and hence $N(k) = (2\pi)^{-3}$.

This result was obtained, by different arguments, by Kasano and Ichimura [29]. A similar result was also obtained by Hussein and McVoy [37]. The alternative derivation presented here, based upon the generalized optical theorem, provides a clear interpretation of this term, as the flux leaving the $x + A$ channel following the breakup of the projectile into $b+x$.

To recapitulate, in the IAV model, the breakup can be viewed as a two-step process. The first step corresponds to the dissociation of the projectile (a) into the fragments b and x , leaving the target in the ground state. The subsequent motion of the participant particle (x) is described by the function $\psi_x^0(\vec{k}_b, \vec{r}_x)$, which is the solution of the inhomogeneous Eq. (12). This particle can then be scattered elastically by the target or can interact non-elastically (for example, excite the target or fuse with it). The former corresponds to the EBU part of the inclusive breakup cross section whereas these non-elastic processes, corresponding to the second step in this two-step picture, yield the NEB contribution. Quantitatively, this contribution is obtained as the expectation value of $\text{Im}[U_x]$ in the state $\psi_x^0(\vec{k}_b, \vec{r}_x)$ [Eq.(24)]. Note that, since this function depends on the final state of the *spectator* particle (b), the NEB expression (24) yields the absorption for each final state of b .

B. Practical implementation of the IAV model

The IAV formula for NEB breakup, Eq. (24), has a deceptively simple form. The function ψ_x^0 must be first calculated from the inhomogeneous Eq. (12), whose source term contains the three-body wave function Ψ^{3b} , which is a complicated object by itself. Furthermore, this equation must be solved for each outgoing energy and angle of b covering the range of interest.

For these reasons, practical implementations of this theory have resorted to additional approximations. Standardly, all these applications rely on the DWBA approximation of the incident channel [that is, Eq. (8)], rather than on a three-body model [Eq. (9)]. Even at the DWBA level, Eq. (12) is not trivial. Usually, a partial wave decomposition of the scattering waves appearing in Eq. (12) will be used and this means that a large number of angular momenta for the $a + A$, $x + A$, and $b + B$ distorted waves will be required for convergence of the calculated cross sections. In addition, the right-hand-side of this equation contains non-local kernels (similar to those appearing in DWBA calculations between bound states, but involving a larger number of angular momenta). Consequently, in addition to the DWBA approximation, most of the existing calculations of this kind have been done in the zero-range (ZR) approximation.

To assess the validity of this approximation, we have performed calculations with both the ZR and exact finite-range (FR) calculations. The detailed formulas for the NEB cross sections in these two approximations are given in the Appendices.

Another difficulty arising in solving Eq. (12) are the well-known convergence problems of the post-form DWBA formula when applied to breakup reactions. This is because $\chi_b^{(-)}$, being a scattering state, will be infinitely oscillatory and the operator in the matrix element V_{bx} and the initial state (ψ_a in DWBA) depend on the \vec{r}_{bx} coordinate and hence there is no natural cutoff in the \vec{r}_b integration. As a consequence, the source term has infinite range. To overcome this problem, Huby and Mines [38] and Vincent [39] multiply the source term by an exponential convergence factor, that damps the contribution of the integral at large distances. Alternatively, following Vincent and Fortune [40], one may use the integration in the complex plane. Here, we adopt a different procedure. Following Thompson [41], we consider energy *bins* for the b distorted waves. For this, the scattering states are first expanded in partial waves (see Appendix A), and the radial coefficients, $R_{\ell_b}(r_b, k_b)$ are then averaged over small energy or momentum intervals, i.e.,

$$\bar{R}_{\ell_b}(r_b, k_b^i) = N \int_{k_b^i - \Delta k_b/2}^{k_b^i + \Delta k_b/2} dk_b R_{\ell_b}(r_b, k_b), \quad (25)$$

where Δk_b is the bin width, k_b^i the central momentum of the bin and N is a normalization constant. The resulting bin wave function is square-integrable and thus leads to convergent results when it is used in the source term of Eq. (12).

The formulas discussed in this section are applied to specific cases in the following section.

III. CALCULATIONS

In this section, we present calculations for several reactions induced by deuterons and ${}^6\text{Li}$ projectiles, and compare the calculated inclusive cross sections with experimental data, in order to assess the validity of the theory. In all cases, we compute the separate contributions for the elastic (EBU) and non-elastic (NEB) breakup cross sections. For the former, we use the CDCC formalism, using the coupled-channels code FRESKO [34]. This permits to treat the EBU to all orders, and should be equivalent to the post-form three-body model of Austern *et al.* For the NEB part, we use the DWBA version of Eq. (24). We have also tested the accuracy of the ZR approximation in the NEB formula, by comparing ZR with FR calculations.

A. Application to (d, pX)

There is a large body of exclusive and inclusive breakup data for deuteron-induced reactions. We have considered the inclusive (d, pX) data for the reactions $d+{}^{93}\text{Nb}$ at $E_d = 25.2$ MeV from Ref. [42], and $d+{}^{58}\text{Ni}$ at 80 and 100 MeV from Refs. [43, 44].

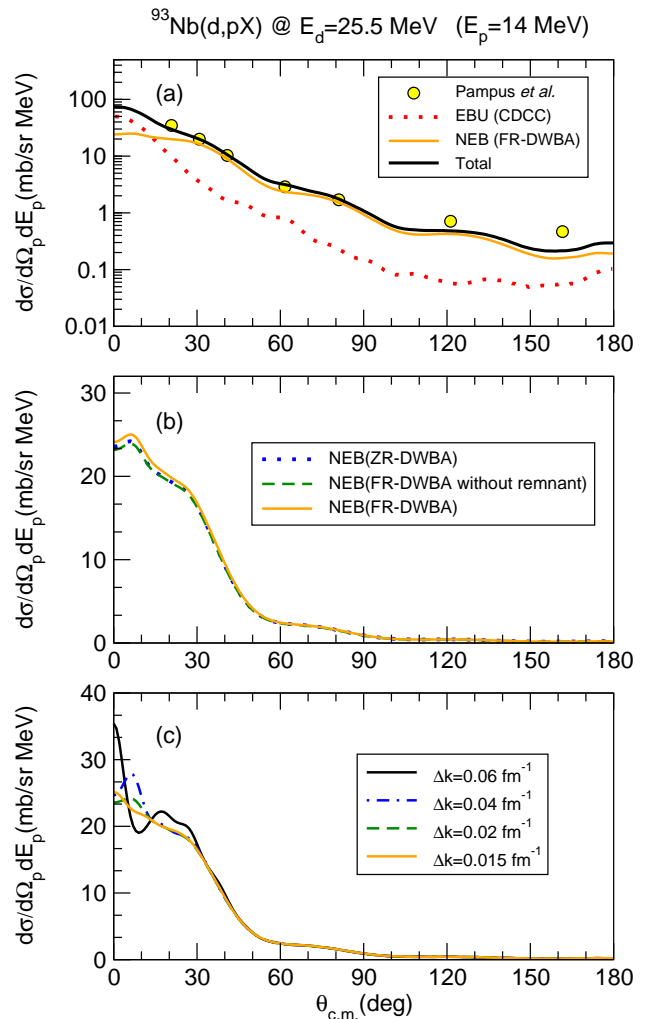


FIG. 2. (Color online) a) Experimental and calculated double differential cross section, as a function of the proton scattering angle, for the protons emitted in the ${}^{93}\text{Nb}(d, pX)$ reaction with an energy of 14 MeV, and a deuteron incident energy of $E_d = 25.5$ MeV. The dotted, thin solid and thick solid lines are the elastic breakup (CDCC), the non-elastic breakup (FR-DWBA) and their incoherent sum, respectively. Experimental data are from Ref. [42]; b) Non-elastic breakup angular distribution calculated with ZR-DWBA (dotted), FR-DWBA without remnant (dashed) and full FR-DWBA (solid line); c) Convergence of the NEB calculation with respect to the bin width, Δk_b , used for the b distorted waves. See text for details.

The data for $d+{}^{93}\text{Nb}$ were already analyzed in Ref. [42], using the so-called surface approximation, in Ref. [29], using the zero-range version of the post-form DWBA formula discussed here, and in Ref. [32], using the prior form of the DWBA IAV model. These calculations give a reasonable account of the experimental data.

In the CDCC calculations [6] the deuteron breakup is treated as inelastic excitations to the p - n continuum. This continuum is truncated at a maximum excitation en-

ergy, and discretized in energy bins. For the present case, the p - n states were included for $\ell = 0 - 4$ partial waves, and up to a maximum excitation energy of 20 MeV. For the p - n interaction, we considered the simple Gaussian form of Ref. [6]. The proton-target and neutron-target interactions were adopted from the global parametrization of Koning and Delaroche (KD) [45], omitting the spin-orbit term, and evaluated at half of the deuteron incident energy. In the CDCC method, the breakup cross sections are calculated in terms of the c.m. scattering angle and excitation energy of the p - n system. Therefore, to compare with the proton inclusive data, these breakup cross sections must be converted to the proton energy and scattering angle, making use of the appropriate kinematical transformation. This was done with the formalism and codes developed in Ref. [46]. For the NEB calculations, we use also the KD parametrization for the proton-target and neutron-target interactions, but evaluated at the corresponding proton (E_p) and neutron (E_n) energies. In DWBA, one needs also the incoming channel optical potential ($d+^{93}\text{Nb}$), which was taken from Ref. [47]. For the ZR-DWBA calculations we used the zero-range constant $D_0 = 125 \text{ MeV} \cdot \text{fm}^{3/2}$, and included the finite-range correction factor (see, e.g., Refs. [48, 49] and Appendix A).

In Fig. 2(a) we compare the experimental [42] and calculated inclusive double differential cross section, $d^2\sigma/dE_p d\Omega_p$, corresponding to a proton energy of $E_p = 14 \text{ MeV}$. The dotted line is the EBU calculation (CDCC), which is found to underestimate the data at all angles. The thin solid line is the FR-DWBA calculation for the NEB part (see Appendix B). The thick solid line is the sum of the EBU and NEB contributions. Except at very large angles, it is found to explain satisfactorily the data. It is seen that, except for the smallest angles, the inclusive breakup cross section is largely dominated by the NEB contribution. Our results are consistent with those reported in Refs. [42] and [29]. In Fig. 2(b), we compare several approximations for the numerical evaluation of the NEB cross section. The dotted line is the ZR-DWBA calculation, including nevertheless the finite-range correction $\Lambda(r_x)$ (see Appendix A). The dashed line is the FR-DWBA calculation, omitting the remnant term in the transition operator (i.e., using $V_{\text{post}} \approx V_{pn}$). Finally, the solid line is the full FR-DWBA calculation. We find that the ZR calculation (with finite-range correction) provides a very accurate result in the present reaction, thus supporting the validity of this approximation in this case. Further, we see that the non-remnant term has a very small effect, and can be also safely ignored in the FR calculation.

In order to obtain meaningful results, the calculated observables must converge as the bin width Δk_b is progressively decreased [c.f. Eq. (25)]. This is verified in Fig. 2(c) for the present case, where we show the calculated NEB angular distribution for different values of Δk_b . Although the rate of convergence was found to be small, it is seen that for $\Delta k_b \approx 0.02 \text{ fm}^{-1}$ the calcula-

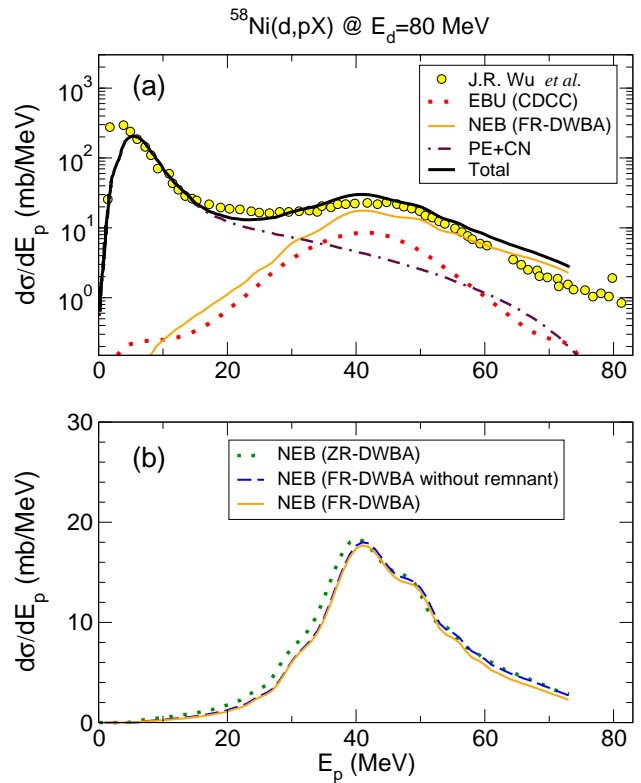


FIG. 3. (Color online)(a) Experimental and calculated angle-integrated proton differential cross section, as a function of the outgoing proton energy in the LAB frame, for the $^{58}\text{Ni}(d,pX)$ reaction at $E_d = 80 \text{ MeV}$. The dotted and thin solid lines are the EBU and NEB contributions, calculated with CDCC and FR-DWBA, respectively. The dot-dashed line is the contribution coming from pre-equilibrium and compound nucleus [50]. The thick solid line is the incoherent sum of the three contributions. Experimental data are from Ref. [43]. (b) Non-elastic breakup calculated with ZR-DWBA (dotted), non-remnant FR-DWBA (dashed), and full FR-DWBA (solid) formulas.

tions are well converged for the full angular range. A similar convergence study was done in the other calculations presented below.

We present now the results for the $^{58}\text{Ni}(d,pX)$ reaction at 80 and 100 MeV, and compare with the data from Refs. [43, 44]. These data have been also analyzed in Refs. [50–52], using the CDCC method for the EBU part, and the semi-classical Glauber approach for the NEB part. In our CDCC calculations, the proton-target and neutron-target interactions are obtained again from the Koning-Delaroche parametrization, and we employed the same p - n interaction used in the $d+^{93}\text{Nb}$ calculations. For the p - n continuum we considered the partial waves $\ell = 0 - 6$, and excitation energies up to 50 MeV and 90 MeV for the data at $E_d = 80 \text{ MeV}$ and $E_d = 100 \text{ MeV}$, respectively. For the NEB calculations, the $d+^{58}\text{Ni}$ potential was taken from Ref. [47].

In Fig. 3, we present the angle-integrated energy dif-

ferential cross section at $E_d=80$ MeV ($d\sigma/dE_p$). In Fig. 3(a), the dotted and thin solid lines correspond to the EBU (CDCC) and NEB (FR-DWBA) calculations. It is seen that the NEB contribution is much larger than the EBU part. Both distributions show a bell-shaped behavior, with a maximum around half of the deuteron energy. However, it is observed that the sum of these two contributions cannot explain the experimental yield at small proton energies. As shown in Ref. [50], these low-energy protons come mainly from compound nucleus followed by evaporation and pre-equilibrium. Since these processes are not accounted for by the present formalism, in this work we have adopted the estimate done in Ref. [50] (dot-dashed line in Fig. 3(a)). The total inclusive cross section, including this contribution (thick solid line) reproduces reasonably well the shape and magnitude of the data. Note that, protons with energies larger than ~ 74 MeV, correspond to bound states of the neutron-target system and they are associated with a stripping mechanism. This contribution could be accommodated in the present formalism solving Eq. (12) for $E_x < 0$ and with boundary conditions appropriate for bound states instead of outgoing boundary conditions. Further, for high-lying bound excited states, were the density of levels will be very high, one may use the ideas of Udagawa and co-workers of extending the complex potential to negative energies to describe the spreading of single-particle states [53, 54]. These extensions go however beyond the scope of the present work.

In Fig. 3(b), we compare different approximations for the transition amplitude used in the NEB calculation, namely, ZR-DWBA (dotted), FR-DWBA with no remnant (dashed) and full FR-DWBA (solid). As in the previous case, the ZR-DWBA and FR-DWBA calculations agree very well for proton energies around and above the maximum, although some small differences are visible. The effect of the remnant term is again found to be very small.

We finally present the results for the $d+^{58}\text{Ni}$ reaction at 100 MeV. This is shown in Fig. 4, where the top panel contains the experimental and calculated proton angular distributions for protons detected at 50 MeV in the laboratory frame, and the bottom panel shows the energy distribution for the protons scattered at 8° in the laboratory frame. Again, it is seen that the inclusive breakup is dominated by the NEB contribution in the full angular range, particularly at large scattering angles. As in the 80 MeV case, both the EBU and NEB contributions exhibit bell-shaped distributions, with a maximum around $\approx E_d/2$. On the other hand, the protons coming from compound nucleus and pre-equilibrium dominate the low-energy region. Except for some underestimation of the cross section at the maximum, the agreement between the theory and the data is rather satisfactory.

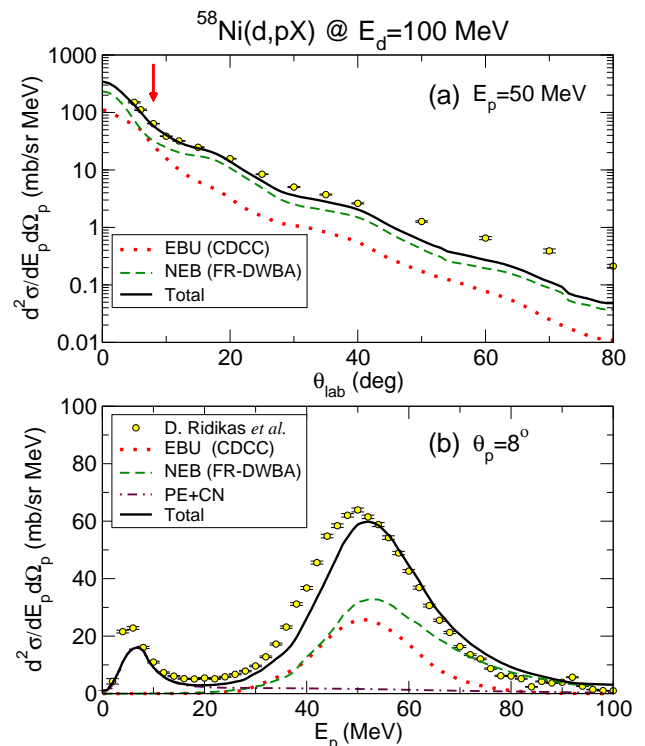


FIG. 4. (Color online) Double differential cross section of protons emitted in the $^{58}\text{Ni}(d,pX)$ reaction at $E_d = 100$ MeV in the laboratory frame. (a) Proton angular distribution for a fixed proton energy of $E_p = 50$ MeV. (b) Energy distribution for protons emitted at a laboratory angle of 8° (arrow in top figure). The meaning of the lines is the same as in Fig. 3, and are also indicated by the labels. Experimental data are from Ref. [44].

B. Application to ($^6\text{Li},\alpha X$)

As a second example, we consider the α production following the breakup of the weakly-bound nucleus ^6Li . The understanding of the large α yields observed in reactions with ^6Li has been subject of many studies [57–65]. These works have shown (see e.g. Refs. [62, 64]) that the total exclusive cross sections ($\alpha+d$ and $\alpha+p$) are much smaller than the total α production cross section. Consequently, the α inclusive cross sections are largely underestimated by CDCC calculations. Furthermore, some of these works have shown that the *total* fusion cross section of these reactions is significantly enhanced due to partial fusion of the projectile, usually referred to as incomplete fusion (ICF) [66]. The calculation of ICF cross sections from a purely quantum mechanical framework is still a challenging problem [66, 67]. Since the ICF is part of the NEB cross section, the inclusive breakup model considered in this work, might provide useful starting point to tackle this problem. However, one has to bear in mind that the NEB cross section will contain, in addition to ICF contributions, other contributions, such as

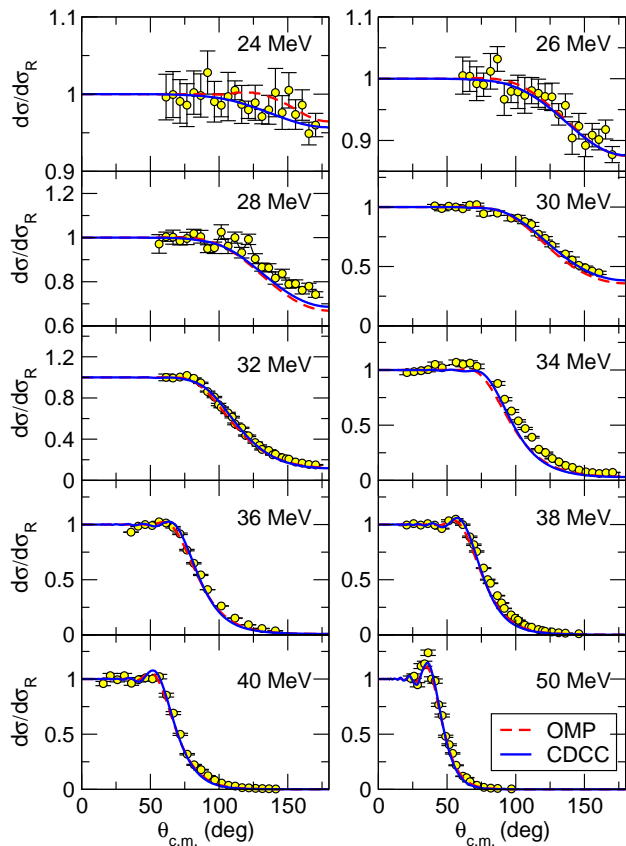


FIG. 5. (Color online) Elastic scattering of ${}^6\text{Li}+{}^{209}\text{Bi}$ at different incident energies. The solid and dashed lines are, respectively, the CDCC calculation and the optical model calculation with the optical potential from [55]. The experimental data are from Ref. [56].

breakup accompanied by target excitation, without absorption of any of the fragments. These contributions should be subtracted from the total NEB cross section in order to extract the ICF part. Work in this direction is in progress and the results will be presented elsewhere. Here, we focus on the calculation of the total inclusive cross sections.

For that purpose, we have considered the ${}^6\text{Li}+{}^{209}\text{Bi}$ reaction at several bombarding energies between 10 and 50 MeV, for which experimental data exist [57]. The nominal Coulomb barrier for this system is around 30.1 MeV [11], so these data cover energies below and above the barrier. The ${}^6\text{Li}$ nucleus is treated in a two-cluster model ($\alpha+d$). CDCC calculations based on this model have been performed for many ${}^6\text{Li}$ induced reactions. In order to reproduce the elastic data, these calculations usually require a reduction of the imaginary part of the fragment-target interactions [68–70]. On the other hand, four-body CDCC calculations, based on a more realistic three-body model of ${}^6\text{Li}$ ($\alpha+p+n$), are able to describe the elastic data for ${}^6\text{Li}+{}^{209}\text{Bi}$ without any readjustment of these potentials [71], thus suggesting that the need for a reduced

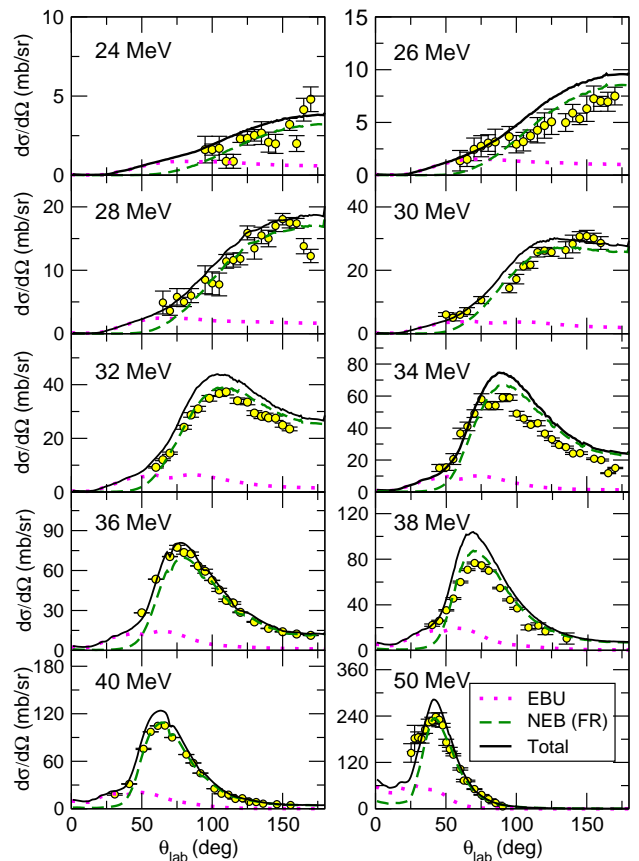


FIG. 6. (Color online) Angular distribution of α particles produced in the reaction ${}^6\text{Li}+{}^{209}\text{Bi}$ at the incident energies indicated by the labels. The dotted, dashed and solid lines correspond to the EBU (CDCC), NEBU (FR-DWBA) and their sum, respectively. Experimental data are from Ref. [57].

absorption is related to the limitations of this two-body model for ${}^6\text{Li}$. Since the inclusive formulas considered in this work are based on a two-body model of the projectile, we perform our calculations with the $\alpha+d$ model, and allow for the same kind of renormalization prescribed in previous works.

For that, we first study the elastic scattering within the CDCC framework. These calculations include s -wave ($J^\pi = 1^+$), p -wave ($J^\pi = 0^-, 1^-, 2^-$), and d -wave ($J^\pi = 1^+, 2^+, 3^+$) continuum states. For the d wave, we make a finer division of bins in order to describe the ${}^6\text{Li}$ resonant states at 2.186 MeV ($J^\pi = 3^+$), 4.31 MeV ($J^\pi = 2^+$) and 5.7 MeV ($J^\pi = 1^+$). For the $\alpha+d$ ground state we used a Woods-Saxon well with $V_0 = 78.46$ MeV, $r_0 = 1.15$ fm, and $a = 0.7$ fm [72]. We used a second Woods-Saxon well to describe the p - and d -wave states with parameters $V_0 = 80.0$ MeV, $r_0 = 1.15$ fm, $a = 0.7$ fm and supplemented with a spin-orbit term, with the usual Woods-Saxon derivative form, and parameters $V_{so} = 2.5$ MeV, $r_{so} = 1.15$ fm, $a_{so} = 0.7$ fm in order to place the d -wave resonances correctly. The d - ${}^{209}\text{Bi}$ and α - ${}^{209}\text{Bi}$ optical potentials are taken from Refs. [73]

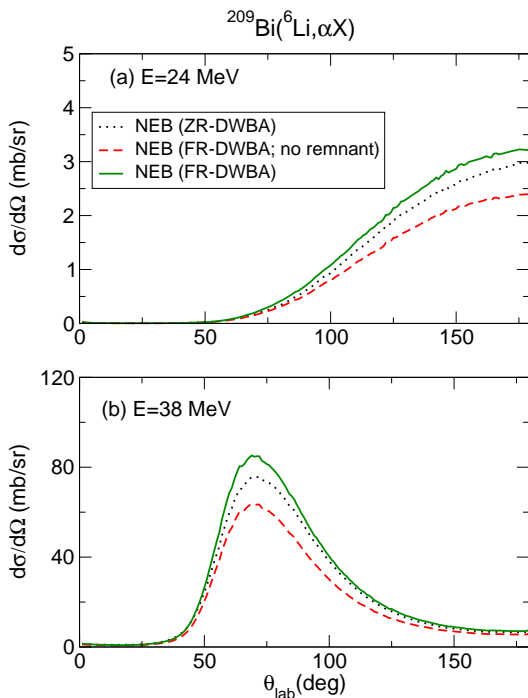


FIG. 7. (Color online) Angular distribution of α particles produced by non-elastic breakup (NEB) in the reaction ${}^6\text{Li}+{}^{209}\text{Bi}$ at the incident energies of (a) 24 MeV and (b) 38 MeV. The dotted, dashed and solid lines are the ZR-DWBA, FR-DWBA without remnant term and full FR-DWBA calculations, respectively.

and [74], respectively. Consistently with previous works, we find that these calculations tend to underestimate the elastic data. We found that, by removing the surface part of the $d-{}^{209}\text{Bi}$ imaginary potential, a good description of the experimental elastic angular distributions is achieved. This is shown in Fig. 5 by solid lines. For comparison, we have included the optical model calculation using the potential of Cook [55] (dashed lines). We note that this reduction of the imaginary potential is consistent with the conclusions of Ref. [71], which points toward an effective suppression of the deuteron breakup in ${}^6\text{Li}$ scattering, compared to the free deuteron scattering.

We discuss now the inclusive breakup cross sections (${}^6\text{Li},\alpha X$). The EBU contribution was obtained from the CDCC calculations discussed above. For the NEB calculations, we used Eq. (24), both in the ZR and FR-DWBA approximations. We adopt the same optical potential of $\alpha/d+{}^{209}\text{Bi}$ as used in the CDCC calculations. For simplicity, the deuteron and target spins are ignored (note that, in the CDCC calculations, the inclusion of the deuteron spin is important to place correctly the $\ell = 2$ resonances). The distorted waves for the incoming channel are calculated with the optical potential of Cook quoted above.

In Fig. 6, we compare the calculated and experimental angular distributions of α particles, for several incident

energies of ${}^6\text{Li}$. The dotted and dashed lines are the EBU (CDCC) and NEB (FR-DWBA) results. Except for the lowest energies, the NEB is found to account for most of the inclusive breakup cross section, in agreement with previous findings [62, 64]. The summed EBU + NEB cross sections (thick solid lines) reproduce fairly well the shape and magnitude of the data, both above and below the barrier. These results give confidence on the possibility of extending the formulation of the IAV theory to situations in which the unobserved particle is a composite system.

At the most forward angles (where the α yield is nevertheless small) the EBU is found to be larger than the NEB part. Using a semi-classical picture, this can be understood by noting that these small angles will correspond to distant trajectories. However, according to Eq. (24), the NEB is only effective for distances within the range of the deuteron-target imaginary potential and hence it will be very small for these distant trajectories. It is worth noting, however, that the separation between EBU and NEB parts in the (${}^6\text{Li},\alpha X$) case is less clear than in the (d,pX) case. In the present model, the NEB is associated with the absorption due to the d -target imaginary potential. If an empirical deuteron-target potential is used, part of this absorption will be due to the breakup of the deuteron into $p+n$. However, in a more realistic description of ${}^6\text{Li}$ in terms of $\alpha+p+n$, the breakup of ${}^6\text{Li}$ into $\alpha+p+n$ (leaving the target in the ground state) would actually correspond to elastic breakup. Despite this ambiguity, we believe that the sum of the two contributions, that is, the TBU cross section, can be reasonably well estimated by the present model, as supported by the comparison with the data.

We study now the validity of the ZR approximation in the present reaction. This is shown in Fig. 7, where we show the angular distribution of α particles produced by NEB, calculated with different DWBA approximations, and at two different energies, one below (24 MeV) and one above (38 MeV) the barrier. The dotted, dashed and solid lines are the ZR-DWBA, FR-DWBA without remnant term and full FR-DWBA results, respectively. We see that the ZR-DWBA calculations underestimate systematically the FR-DWBA results by about $\sim 10 - 20\%$ and hence the validity of the ZR approximation is more questionable than in the deuteron case. Further, we find that the no-remnant FR-DWBA calculation underestimates the full FR-DWBA result by about $\sim 30 - 40\%$, indicating that the effect of the remnant term is much more important than in the deuteron case, owing to the strong Coulomb interaction and the difference of the geometry, \vec{r}_{bA} and \vec{r}_b , caused by the valence particle.

Finally, we study the incident energy dependence of the total α yield. This is shown in Fig. 8. The squares and the open circles correspond, respectively, to the NEB (FR-DWBA) and EBU (CDCC) contributions to the α production cross section. At energies above the nominal Coulomb barrier (indicated by the arrow) the NEB largely dominates the inclusive breakup. Below the

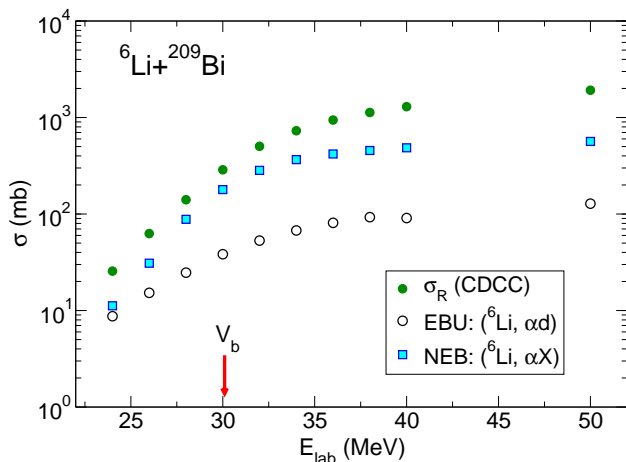


FIG. 8. (Color online) Integrated cross sections for the reaction ${}^6\text{Li}$ on ${}^{209}\text{Bi}$ as a function of the incident laboratory energy. The open circles and the squares are the EBU (CDCC) and NEB (FR-DWBA) contributions to the α inclusive cross section. The solid circles are the reaction cross sections, obtained from the CDCC calculations. The arrow indicates the nominal position of the Coulomb barrier.

Coulomb barrier, both contributions become comparable. This can be again explained in classical terms, by noting that, at these small energies, the distance of closest approach will be relatively large, due to the presence of the Coulomb barrier and, therefore, the imaginary part of the d +target potential (which is responsible for the NEB part) will have little effect. We have included in the same plot the total reaction cross sections, as extracted from the CDCC calculations, which are found to be very close to the values calculated with the Cook optical potential (not shown). It is seen that, at energies below the Coulomb barrier, the reaction cross section is almost exhausted by the $({}^6\text{Li}, \alpha X)$ TBU cross section, whereas at energies above the Coulomb barrier other processes beyond the breakup seem to be present (e.g. pure target excitation, α absorption, complete fusion, etc). A more detailed analysis of these processes is under study and will be presented elsewhere.

IV. SUMMARY AND CONCLUSIONS

In summary, we have addressed the problem of the calculation of inclusive breakup in reactions induced by weakly-bound projectiles. For that purpose, we have revisited the model proposed by Ichimura, Austern and Vincent in the eighties [6, 30]. We have presented an alternative derivation of the non-elastic breakup (NEB) formula, based on a direct application of the coupled-channels optical theorem, which provides a transparent interpretation of the NEB as the part of the flux that leaves the elastic breakup channels to more complicated configurations of the $x+A$ system.

Using the DWBA version of this formula, for the NEB, and the CDCC framework, for the EBU part, we have performed calculations for deuteron and ${}^6\text{Li}$ reactions on several targets, and at different energies, finding a satisfactory agreement with the available inclusive breakup data in all the cases considered. These calculations show that, except for the particles emitted at small angles, most of the inclusive breakup corresponds to NEB. We have also tested the validity of the zero-range approximation and the effect of the remnant term in the NEB calculation, by comparing with exact finite-range DWBA calculations. For the studied deuteron reactions, the effect of the remnant term has been found to be very small and the zero-range calculation gives a result very close to the full finite-range calculation. On the other hand, for the ${}^6\text{Li}+{}^{209}\text{Bi}$ reaction, finite-range effects become important and should be therefore considered for a correct interpretation of experimental data.

The good agreement between the calculated inclusive cross sections and the data suggests that this approach could be also useful to estimate the amount of incomplete fusion (ICF) from the inclusive breakup. This problem is of interest, for instance, in surrogate nuclear reactions studies [17]. The separation of complete from ICF has been also pointed out to be essential for the extraction of meaningful conclusions regarding the effect of breakup on fusion [75]. To answer these problems in a quantitatively way, one needs to extend the present model in order to disentangle the ICF part from other NEB channels, such as transfer to bound states or target excitation.

An interesting question that arises is how these results depend on the incident energy, the mass of the target and the separation energy of the projectile. Further calculations are in progress in order to answer these questions. In particular, in the case of the scattering of very weakly-bound projectiles with heavy targets, there are evidences that the EBU component can be dominant [76, 77]. A proper understanding of these reactions, however, may require going beyond the DWBA approximation adopted here for the NEB calculations. For that, the three-body model of Austern *et al.* may provide an adequate framework and, hence, its implementation is currently under investigation.

ACKNOWLEDGMENTS

We are grateful to Prof. H. Wolter for a critical reading of the manuscript. This work has been partially supported by the Spanish Ministerio de Economía y Competitividad, under grant FIS2013-41994-P, by the Spanish Consolider-Ingenio 2010 Programme CPAN (CSD2007-00042) and by Junta de Andalucía (FQM160, P07-FQM-02894). J.L. is partially supported by a grant funded by the China Scholarship Council.

Appendix A: Nonelastic breakup formula in the zero-range approximation

In DWBA, the source term of Eq. (12) can be written as

$$\rho(\vec{k}_b, \vec{r}_x) = (\chi_b^{(-)} | V_{\text{post}} | \chi_a^{(+)} \phi_a), \quad (\text{A1})$$

with $V_{\text{post}} \equiv V_{bx} + U_{bA} - U_{bB}$ and where we have omitted the dependence on \vec{k}_a for simplicity of the notation. The symbol $(|)$ means that the integration is to be taken over all the coordinates except the x -channel coordinate \vec{r}_x . If the remnant term $U_{bA} - U_{bB}$ is small, $\phi_a(\vec{r}_{bx})$ corresponds to an s -wave and V_{bx} is short-ranged, the integral is dominated by the values $r_{bx} \approx 0$ and can be evaluated in the zero-range approximation, i.e.,

$$V_{\text{post}} \phi_a(\vec{r}_{bx}) \simeq V_{bx}(r_{bx}) \phi_a(\vec{r}_{bx}) \simeq D_0 \delta(\vec{r}_{bx}), \quad (\text{A2})$$

where D_0 is the *zero-range constant*. Using this approximation in (A1), and including the so-called *finite-range correction* (see, for instance, Sec. 6.14 of Ref. [49]) the source term results

$$\rho(\vec{k}_b, \vec{r}_x) = D_0 \chi_b^{(-)*}(\vec{k}_b, c\vec{r}_x) \chi_a^{(+)}(\vec{k}_a, \vec{r}_x) \Lambda(r_x), \quad (\text{A3})$$

where $c = m_A/(m_A + m_x)$ and $\Lambda(r_x)$ is the *finite-range correction factor*.

Ignoring the internal spins of the colliding particles, the distorted waves can be expanded as

$$\chi^{(+)}(\vec{k}, \vec{r}) = \frac{4\pi}{kr} \sum_{lm} i^l R_l(r) Y_l^m(\hat{r}) Y_l^{m*}(\hat{k}). \quad (\text{A4})$$

For charged particles, the radial part is here assumed to include the Coulomb phase, $e^{i\sigma_l}$, where σ_l are the Coulomb phase shifts.

Following [29], the source term is expanded in spherical

$$\mathfrak{J}_{l_x m_x}(\vec{k}_a, \vec{k}_b) = \int dr W_x(r_x) \left| \sum_{l_a} \sum_{l_b} \mathfrak{R}_{l_x}^{l_a l_b}(r_x) \mathfrak{Y}_{l_x m_x}^{l_a l_b}(\hat{k}_a, \hat{k}_b) \right|^2 \quad (\text{A13})$$

Appendix B: Nonelastic breakup formula in the finite-range approximation

In the finite-range approximation, the source term (A1) is evaluated exactly. Because all the relevant coor-

harmonics as

$$\begin{aligned} \rho(\vec{k}_b, \vec{r}_x) &= \frac{16\pi^2}{k_a k_b} \sum_{l_x m_x} Y_{l_x}^{m_x}(\hat{r}_x) \\ &\times \sum_{l_a} \sum_{l_b} \rho_{l_x}^{l_a l_b}(r_x) \mathfrak{Y}_{l_x m_x}^{l_a l_b}(\hat{k}_a, \hat{k}_b) \end{aligned} \quad (\text{A5})$$

with

$$\begin{aligned} \rho_{l_x}^{l_a l_b}(r_x) &= \frac{D_0}{c r_x^2} i^{l_a + l_b} (-1)^{l_b} \left[\frac{(2l_a + 1)(2l_b + 1)}{4\pi(2l_x + 1)} \right]^{1/2} \\ &\times \langle l_a l_b 00 | l_x 0 \rangle R_{l_a}(r_x) R_{l_b}(c r_x) \Lambda(r_x) \end{aligned} \quad (\text{A6})$$

and

$$\mathfrak{Y}_{l_x m_x}^{l_a l_b}(\hat{k}_a, \hat{k}_b) = \sum_{m_a m_b} \langle l_a l_b m_a m_b | l_x m_x \rangle Y_{l_b}^{m_b*}(\hat{k}_b) Y_{l_a}^{m_a*}(\hat{k}_a) \quad (\text{A7})$$

The channel wave function $\psi_x^0(\vec{k}_b, \vec{r}_x)$ in Eq. (12) is also expanded in spherical harmonics

$$\psi_x^0(\vec{k}_b, \vec{r}_x) = \frac{16\pi^2}{k_a k_b} \frac{1}{r_x} \sum_{l_x m_x} \psi_{l_x m_x}^0(r_x, \vec{k}_a, \vec{k}_b) Y_{l_x m_x}(\hat{r}_x) \quad (\text{A8})$$

For convenience, $\psi_{l_x m_x}^0(r_x, \vec{k}_a, \vec{k}_b)$ is written as

$$\psi_{l_x m_x}^0(r_x, \vec{k}_a, \vec{k}_b) = \sum_{l_a} \sum_{l_b} \mathfrak{R}_{l_x}^{l_a l_b}(r_x) \mathfrak{Y}_{l_x m_x}^{l_a l_b}(\hat{k}_a, \hat{k}_b). \quad (\text{A9})$$

Inserting the expansions (A6) and (A9) into the inhomogeneous equation Eq. (12), one gets

$$\left\{ \frac{\hbar^2}{2\mu_x} \left[\frac{d^2}{dr_x^2} - \frac{l_x(l_x + 1)}{r_x^2} \right] - U_x + E_x \right\} \mathfrak{R}_{l_x}^{l_a l_b}(r_x) = r_x \rho_{l_x}^{l_a l_b}(r_x) \quad (\text{A10})$$

For $E_x > 0$ (unbound x -A states), this equation is to be solved with outgoing boundary conditions

$$\mathfrak{R}_{l_x}^{l_a l_b}(r_x) \rightarrow -S_{l_x}^{l_a l_b} H_{l_x}^{(+)}(k_x r_x) \quad (\text{A11})$$

where $H_{l_x}^{(+)}(k_x r_x)$ is a Coulomb outgoing wave and the coefficients $S_{l_x}^{l_a l_b}$ are the S-matrix elements.

Finally, the double differential cross section of nonelastic breakup with zero-range approximation results

$$\left[\frac{d^2\sigma}{d\Omega_b dE_b} \right]_{\text{post}}^{\text{NEB}} = \frac{64\pi\mu_a\mu_b}{\hbar^4 k_a^3 k_b} \sum_{l_x m_x} \mathfrak{J}_{l_x m_x}(\vec{k}_a, \vec{k}_b) \quad (\text{A12})$$

where

dinates lie on the same plane (see Fig. 1), one can express

any coordinate in terms of two independent vectors. So, for example, choosing \vec{r}_x and \vec{r}_b as independent vectors, one may write

$$\vec{r}_{bx} = q\vec{r}_x - \vec{r}_b \quad \text{and} \quad \vec{r}_a = (1-pq)\vec{r}_x + p\vec{r}_b \quad (\text{B1})$$

where $p = m_b/(m_b + m_x)$ and $q = m_A/(m_A + m_x)$. The projectile wave function, neglecting again its internal spin, can be expressed as $\phi_a(\vec{r}_{bx}) = (R_{l_{bx}}(r_{bx})/r_{bx})Y_{l_{bx}}^{m_{bx}}(\hat{r}_{bx})$. Using this, and the partial wave decomposition of the distorted waves, the source term is written as

$$\begin{aligned} \rho_b^{m_{bx}}(\vec{k}_b, \vec{r}_x) &= \frac{16\pi^2}{k_a k_b} \sum_{l_a m_a} \sum_{l_b m_b} i^{l_a + l_b} (-1)^{l_b} Y_{l_b}^{m_b*}(\hat{k}_b) \\ &\times Y_{l_a}^{m_a*}(\hat{k}_a) \int d\vec{r}_b V_{\text{post}} \frac{R_{l_b}(r_b)}{r_b} Y_{l_b}^{m_b}(\hat{r}_b) \\ &\times \frac{R_{l_a}(r_a)}{r_a} Y_{l_a}^{m_a}(\hat{r}_a) \frac{R_{l_{bx}}(r_{bx})}{r_{bx}} Y_{l_{bx}}^{m_{bx}}(\hat{r}_{bx}) \end{aligned} \quad (\text{B2})$$

$$Y_{l_{bx}}^{m_{bx}}(\hat{r}_{bx}) = \sqrt{4\pi} \sum_{n=0}^{l_{bx}} \sum_{\lambda=-n}^n c(l_{bx}, n) \frac{(qr_x)^{l_{bx}-n} (-r_b)^n}{r_{bx}^{l_{bx}}} Y_{l_{bx}-n}^{m_{bx}-\lambda}(\hat{r}_x) Y_n^\lambda(\hat{r}_b) \langle l_{bx}-n, n, m_{bx}-\lambda, \lambda | l_{bx}, m_{bx} \rangle, \quad (\text{B3})$$

$$Y_{l_a}^{m_a}(\hat{r}_a) = \sqrt{4\pi} \sum_{u=0}^{l_a} \sum_{\nu=-u}^u c(l_a, u) \frac{(pr_b)^{l_a-u} (1-pq)^u (r_x)^u}{r_a^{l_a}} Y_{l_a-u}^{m_a-\nu}(\hat{r}_b) Y_u^\nu(\hat{r}_x) \langle l_a-u, u, m_a-\nu, \nu | l_a, m_a \rangle, \quad (\text{B4})$$

where

$$c(x, y) = \left(\frac{(2x+1)!}{(2y+1)!(2(x-y)+1)!} \right)^{1/2} \quad (\text{B5})$$

Because the interaction V_{post} is an scalar, we can perform the Legendre expansion

$$V_{\text{post}} \frac{R_{l_a}(r_a)}{(r_a)^{l_a+1}} \frac{R_{l_{bx}}(r_{bx})}{(r_{bx})^{l_{bx}+1}} = \sum_{T=0}^{T_{max}} (2T+1) \mathbf{q}_{l_a, l_{bx}}^T(r_b, r_x) P_T(z) \quad (\text{B6})$$

We note that, even if a finite-range treatment is made, in reactions of light projectiles on heavy targets (e.g., deuteron scattering on heavy targets), the difference $U_{bA} - U_{bB}$, known as *remnant term*, can be neglected, and thus $V_{\text{post}} \simeq V_{bx}$. The limit T_{max} is chosen large enough to generate all the couplings for partial waves to be used. Here, the argument z in the Legendre polynomials $P_T(z)$ is the cosine of the angle between \vec{r}_b and \vec{r}_x . The radial kernels are explicitly given by

$$\mathbf{q}_{l_a, l_{bx}}^T(r_b, r_x) = \frac{1}{2} \int_{-1}^1 V_{\text{post}} \frac{R_{l_a}(r_a)}{(r_a)^{l_a+1}} \frac{R_{l_{bx}}(r_{bx})}{(r_{bx})^{l_{bx}+1}} P_T(z) dz. \quad (\text{B7})$$

To calculate this, we transform the spherical harmonics $Y_{l_a}^{m_a}(\hat{r}_a)$ and $Y_{l_{bx}}^{m_{bx}}(\hat{r}_{bx})$ into linear combinations of the spherical harmonics $Y_{l_b}^{m_b}(\hat{r}_b)$ and $Y_{l_x}^{m_x}(\hat{r}_x)$. This is done by means of the Moshinsky solid-harmonic expansion [78]

Finally, the source term results

$$\begin{aligned} \rho_b^{m_{bx}}(\vec{k}_b, \vec{r}_x) &= \frac{16\pi^2}{k_a k_b} \sum_{l_x m_x} Y_{l_x}^{m_x}(\hat{r}_x) \\ &\times \sum_{l_a l_b} \sum_l \mathfrak{Y}_{l_a l_b}^{l_x m_x m_{bx}}(\hat{k}_a, \hat{k}_b) \rho_{l_x}^{l_a l_b}(r_x), \end{aligned} \quad (\text{B8})$$

with

$$\begin{aligned} \mathfrak{Y}_{l_a l_b}^{l_x m_x m_{bx}}(\hat{k}_a, \hat{k}_b) &= \sum_{m_a m_b} Y_{l_a}^{m_a*}(\hat{k}_a) Y_{l_b}^{m_b*}(\hat{k}_b) \\ &\times \langle l_a l_{bx} m_a m_{bx} | l m_l \rangle \langle l l_b m_l m_b | l_x m_x \rangle, \end{aligned} \quad (\text{B9})$$

and

$$\begin{aligned}
\rho_{l_x}^{l_a l_b}(r_x) &= \sum_{nu} \sum_{\Lambda_a \Lambda_b} \sum_T i^{l_a + l_b} (-1)^{l_b + l + n + \Lambda_b - \Lambda_a} p^{l_a - u} \\
&\times (qr_x)^{l_{bx} - n} (r_x)^u (1 - pq)^u \widehat{l_a - u} \widehat{l_{bx} - n} \widehat{n} \widehat{n} \widehat{u} \\
&\times \hat{l}_{bx} \hat{\Lambda}_a \hat{\Lambda}_b \hat{l}_a \hat{l}_b \hat{T} / \hat{l}_x c(l_{bx}, n) c(l_a, u) \\
&\times \langle u, l_{bx} - n, 00 | \Lambda_b 0 \rangle \langle l_a - u, n, 0, 0 | \Lambda_a, 0 \rangle \\
&\times \langle \Lambda_b, T, 0, 0 | l_x, 0 \rangle \langle \Lambda_a, l_b, 0, 0 | T, 0 \rangle (2l + 1) \\
&\times \begin{Bmatrix} l_{bx} & l & l_a \\ n & \Lambda_a & l_a - u \\ l_{bx} - n & \Lambda_b & u \end{Bmatrix} W(l_x, \Lambda_b, l_b, \Lambda_a; T, l) \\
&\times \int dr_b R_{l_b}(r_b) (r_b)^{l_a - u + n + 1} \mathbf{q}_{l_a, l_{bx}}^T(r_b, r_x)
\end{aligned} \tag{B10}$$

As in the zero-range case, $\psi_x^0(\vec{k}_b, \vec{r}_x)$ can be expanded as

$$\begin{aligned}
\psi_x^0(\vec{k}_b, \vec{r}_x) &= \frac{16\pi^2}{k_a k_b} r_x^{-1} \sum_{l_x m_x} Y_{l_x}^{m_x}(\hat{r}_x) \\
&\times \sum_{l_a l_b} \sum_l \mathfrak{R}_{l_x}^{l_a l_b}(r_x) \mathfrak{Y}_{l_a l_b}^{l_x m_x m_{bx}}(\hat{k}_a, \hat{k}_b) \tag{B11}
\end{aligned}$$

where the radial coefficients, $\mathfrak{R}_{l_x}^{l_a l_b}(r_x)$, are solutions of the inhomogeneous equation

$$\left\{ \frac{\hbar^2}{2\mu_x} \left[\frac{d^2}{dr_x^2} - \frac{l_x(l_x + 1)}{r_x^2} \right] - U_x + E_x \right\} \mathfrak{R}_{l_x}^{l_a l_b}(r_x) = r_x \rho_{l_x}^{l_a l_b}(r_x) \tag{B12}$$

The boundary condition is the same as in the zero-range case.

Finally, the double differential cross section with finite range post-form DWBA can be written as

$$\left[\frac{d^2\sigma}{d\Omega_b dE_b} \right]_{\text{post}}^{\text{NEB}} = \frac{64\pi\mu_a\mu_b}{\hbar^4 k_a^3 k_b} \frac{1}{2l_{bx} + 1} \sum_{l_x m_x} \mathfrak{J}_{l_x m_x}^{m_{bx}}(\vec{k}_a, \vec{k}_b) \tag{B13}$$

with

$$\mathfrak{J}_{l_x m_x}^{m_{bx}}(\vec{k}_a, \vec{k}_b) = \int dr_x W_x(r_x) \left| \sum_{l_a l_b l} \mathfrak{R}_{l_x}^{l_a l_b}(r_x) \mathfrak{Y}_{l_a l_b}^{l_x m_x m_{bx}}(\hat{k}_a, \hat{k}_b) \right|^2 \tag{B14}$$

-
- [1] T. Nakamura *et al.*, Phys. Rev. Lett. **103**, 262501 (2009).
 - [2] T. Nakamura and Y. Kondo, in *Lecture Notes in Physics 848 Vol 2.*, edited by C. Beck (Springer Berlin, 2012) p. 67.
 - [3] L. D. Faddeev, Zh. Eksp. Teor. Fiz. **39**, 1459 (1960), [Sov. Phys. JETP **12**, 1014 (1961)].
 - [4] W. Glöckle, *The Quantum Mechanical Few-Body Problem* (Springer-Verlag, Berlin/Heidelberg, 1983).
 - [5] G. Baur, R. Shyam, F. Rösler, and D. Trautmann, Phys. Rev. C **28**, 946 (1983).
 - [6] N. Austern, Y. Iseri, M. Kamimura, M. Kawai, G. Raritscher, and M. Yahiro, Phys. Rep. **154**, 125 (1987).
 - [7] S. Typel and G. Baur, Phys. Rev. **C50**, 2104 (1994).
 - [8] H. Esbensen and G. F. Bertsch, Nucl. Phys. **A600**, 37 (1996).
 - [9] T. Kido, K. Yabana, and Y. Suzuki, Phys. Rev. **C 50**, R1276 (1994).
 - [10] P. Capel, G. Goldstein, and D. Baye, Phys. Rev. **C 70**, 064605 (2004).
 - [11] M. Dasgupta *et al.*, Phys. Rev. **C66**, 041602 (2002).
 - [12] L. F. Canto, R. Donangelo, L. M. de Matos, M. S. Hussein, and P. Lotti, Phys. Rev. **C58**, 1107 (1998).
 - [13] M. S. Hussein, B. V. Carlson, T. Frederico, and T. Tarutina, Nucl. Phys. **A738**, 367 (2004).
 - [14] S. Hashimoto, K. Ogata, S. Chiba, and M. Yahiro, Progress of Theoretical Physics **122**, 1291 (2009).
 - [15] M. Boselli and A. Diaz-Torres, Journal of Physics G: Nuclear and Particle Physics **41**, 094001 (2014).
 - [16] I. Thompson and A. Diaz-Torres, Progress of Theoretical Physics Supplement **154**, 69 (2004).
 - [17] J. E. Escher, J. T. Burke, F. S. Dietrich, N. D. Scielzo, I. J. Thompson, and W. Younes, Rev. Mod. Phys. **84**, 353 (2012).
 - [18] A. M. Moro, R. Crespo, H. Garcia-Martinez, E. F. Aguilera, E. Martinez-Quiroz, J. Gomez-Camacho, and F. M. Nunes, Phys. Rev. **C 68**, 034614 (2003).
 - [19] D. Escrig *et al.*, Nucl. Phys. **A792**, 2 (2007).
 - [20] P. N. de Faria, R. Lichtenthäler, K. C. C. Pires, A. M. Moro, A. Lépine-Szily, V. Guimarães, D. R. Mendes, A. Arazi, A. Barioni, V. Morcelle, and M. C. Morais, Phys. Rev. **C 82**, 034602 (2010).
 - [21] J. A. Tostevin, Nucl. Phys. **A682**, 320c (2001).
 - [22] P. G. Hansen and J. A. Tostevin, Ann. Rev. Nucl. Part. Sci. **53**, 219 (2003).
 - [23] A. Budzanowski, G. Baur, C. Alderliesten, J. Bojowald, C. Mayer-Boricke, W. Oelert, P. Turek, F. Rosel, and D. Trautmann, Phys. Rev. Lett. **41**, 635 (1978).

- [24] G. Baur, R. Shyam, F. Rosel, and D. Trautmann, Phys. Rev. **C21**, 2668 (1980).
- [25] R. Shyam, G. Baur, F. Rosel, and D. Trautmann, Phys. Rev. **C22**, 1401 (1980).
- [26] T. Udagawa and T. Tamura, Phys. Rev. C **24**, 1348 (1981).
- [27] T. Udagawa, X. H. Li, and T. Tamura, Phys. Lett. **135B**, 333 (1984).
- [28] N. Austern and C. M. Vincent, Phys. Rev. C **23**, 1847 (1981).
- [29] A. Kasano and M. Ichimura, Phys. Lett. **115B**, 81 (1982).
- [30] M. Ichimura, N. Austern, and C. M. Vincent, Phys. Rev. C **32**, 431 (1985).
- [31] B. V. Carlson, R. Capote, and M. Sin, arXiv:1508.01466 (2015).
- [32] G. Potel, F. M. Nunes, and I. J. Thompson, Phys. Rev. C **92**, 034611 (2015).
- [33] R. J. Ascutto and N. K. Glendenning, Phys. Rev. **181**, 1396 (1969).
- [34] I. J. Thompson, Comp. Phys. Rep. **7**, 167 (1988).
- [35] M. L. Goldberger and K. M. Watson, *Collision theory* (Courier Dover Publications, 2004).
- [36] S. R. Cotanch, Nucl. Phys. **A842**, 48 (2010).
- [37] M. Hussein and K. McVoy, Nucl. Phys. A **445**, 124 (1985).
- [38] R. Huby and J. R. Mines, Rev. Mod. Phys. **37**, 406 (1965).
- [39] C. M. Vincent, Phys. Rev. **175**, 1309 (1968).
- [40] C. M. Vincent and H. T. Fortune, Phys. Rev. C **2**, 782 (1970).
- [41] I. J. Thompson, J. Phys.: Conf. Ser. **312**, 082041 (2011).
- [42] J. Pampus, J. Bisplinghoff, J. Ernst, T. Mayer-Kuckuk, J. Rama Rao, G. Baur, F. Rosel, and D. Trautmann, Nucl. Phys. **A311**, 141 (1978).
- [43] J. R. Wu, C. C. Chang, and H. D. Holmgren, Phys. Rev. C **19**, 370 (1979).
- [44] D. Ridikas, W. Mittig, H. Savajols, P. Roussel-Chomaz, S. V. Förtlisch, J. J. Lawrie, and G. F. Steyn, Phys. Rev. C **63**, 014610 (2000).
- [45] A. Koning and J. Delaroche, Nucl. Phys. A **713**, 231 (2003).
- [46] J. A. Tostevin, F. M. Nunes, and I. J. Thompson, Phys. Rev. C **63**, 024617 (2001).
- [47] H. An and C. Cai, Phys. Rev. C **73**, 054605 (2006).
- [48] P. Buttle and L. B. Goldfarb, Proceedings of the Physical Society **83**, 701 (1964).
- [49] G. Satchler, *Direct nuclear reactions*, International series of monographs on physics (Clarendon Press, 1983).
- [50] W. Jia, Y. Tao, S. Wei-Li, Y. Watanabe, and K. Ogata, Chinese Physics Letters **28**, 112401 (2011).
- [51] T. Ye, S. Hashimoto, Y. Watanabe, K. Ogata, and M. Yahiro, Phys. Rev. C **84**, 054606 (2011).
- [52] S. Nakayama, S. Araki, Y. Watanabe, O. Iwamoto, T. Ye, and K. Ogata, Nuclear Data Sheets **118**, 305 (2014).
- [53] T. Udagawa, Y. J. Lee, and T. Tamura, Phys. Lett. **196B**, 291 (1987).
- [54] T. Udagawa, Y. J. Lee, and T. Tamura, Phys. Rev. **C39**, 47 (1989).
- [55] J. Cook, Nucl. Phys. A **388**, 153 (1982).
- [56] S. Santra, S. Kailas, K. Ramachandran, V. V. Parkar, V. Jha, B. J. Roy, and P. Shukla, Phys. Rev. C **83**, 034616 (2011).
- [57] S. Santra, S. Kailas, V. V. Parkar, K. Ramachandran, V. Jha, A. Chatterjee, P. K. Rath, and A. Parihari, Phys. Rev. C **85**, 014612 (2012).
- [58] K. Pfeiffer, E. Speth, and K. Bethge, Nucl. Phys. A **206**, 545 (1973).
- [59] C. M. Castaneda, H. A. Smith, P. P. Singh, and H. Karwowski, Phys. Rev. C **21**, 179 (1980).
- [60] G. R. Kelly, N. J. Davis, R. P. Ward, B. R. Fulton, G. Tungate, N. Keeley, K. Rusek, E. E. Bartosz, P. D. Cathers, D. D. Caussyn, T. L. Drummer, and K. W. Kemper, Phys. Rev. C **63**, 024601 (2000).
- [61] A. Pakou, N. Alamanos, A. Gillibert, M. Kokkoris, S. Kossionides, A. Lagoyannis, N. G. Nicolis, C. Papachristodoulou, D. Patiris, D. Pierrotsakou, E. C. Polacco, and K. Rusek, Phys. Rev. Lett. **90**, 202701 (2003).
- [62] C. C. Signorini *et al.*, Phys. Rev. C **67**, 044607 (2003).
- [63] F. Souza *et al.*, Nucl. Phys. A **821**, 36 (2009).
- [64] H. Kumawat, V. Jha, V. V. Parkar, B. J. Roy, S. Santra, V. Kumar, D. Dutta, P. Shukla, L. M. Pant, A. K. Mohanty, R. K. Choudhury, and S. Kailas, Phys. Rev. C **81**, 054601 (2010).
- [65] M. K. Pradhan, A. Mukherjee, S. Roy, P. Basu, A. Goswami, R. Kshetri, R. Palit, V. V. Parkar, M. Ray, M. Saha Sarkar, and S. Santra, Phys. Rev. C **88**, 064603 (2013).
- [66] L. Canto, P. Gomes, R. Donangelo, and M. Hussein, Phys. Rep. **424**, 1 (2006).
- [67] H. D. Marta, L. F. Canto, and R. Donangelo, Phys. Rev. C **89**, 034625 (2014).
- [68] Y. Hirabayashi and Y. Sakuragi, Phys. Lett. B **258**, 11 (1991).
- [69] C. Beck, N. Keeley, and A. Diaz-Torres, Phys. Rev. C **75**, 054605 (2007).
- [70] S. Santra *et al.*, Phys. Lett. B **677**, 139 (2009).
- [71] S. Watanabe, T. Matsumoto, K. Minomo, K. Ogata, and M. Yahiro, Phys. Rev. C **86**, 031601 (2012).
- [72] H. Nishioka, J. Tostevin, R. Johnson, and K.-I. Kubo, Nucl. Phys. A **415**, 230 (1984).
- [73] Y. Han, Y. Shi, and Q. Shen, Phys. Rev. C **74**, 044615 (2006).
- [74] A. R. Barnett and J. S. Lilley, Phys. Rev. C **9**, 2010 (1974).
- [75] M. Dasgupta *et al.*, Phys. Rev. C **70**, 024606 (2004).
- [76] A. Di Pietro *et al.*, Phys. Rev. C **85**, 054607 (2012).
- [77] J. Fernandez-Garcia *et al.*, Phys. Rev. Lett. **110**, 142701 (2013).
- [78] M. Moshinsky, Nucl. Phys. **13**, 104 (1959).